A Journal of the Gesellschaft Deutscher Chemiker

Angewandte International Edition Chemie

GDCh

www.angewandte.org

Accepted Article

Title: Dynamic Control of Chiral Space Through Local Symmetry Breaking in a Rotaxane Organocatalyst

Authors: Marcel Dommaschk, Javier Echavarren, David Leigh, Vanesa Marcos, and Thomas A Singleton

To be cited as: *Angew. Chem. Int. Ed.* 10.1002/anie.201908330
Angew. Chem. 10.1002/ange.201908330

Link to VoR: http://dx.doi.org/10.1002/anie.201908330
http://dx.doi.org/10.1002/ange.201908330

WILEY-VCH

10.1002/anie.201908330

WILEY-VCH

COMMUNICATION

Dynamic Control of Chiral Space Through Local Symmetry Breaking in a Rotaxane Organocatalyst

Marcel Dommaschk, Javier Echavarren, David A. Leigh,* Vanesa Marcos and Thomas A. Singleton

Abstract We report on a switchable rotaxane molecular shuttle that features a pseudo-*meso* 2,5-disubstituted pyrrolidine catalytic unit on the axle whose local symmetry is broken according to the position of a threaded benzylic amide macrocycle. The macrocycle can be selectively switched with high fidelity (with light in one direction; with catalytic acid in the other) between binding sites located to either side of the pyrrolidine unit. The position of the macrocycle dictates the facial bias of the rotaxane-catalyzed conjugate addition of aldehydes to vinyl sulfones. The pseudo-*meso* non-interlocked thread does not afford significant selectivity as a catalyst (2-14 % ee), whereas the rotaxane affords selectivities of up to 40 % ee with switching of the position of the macrocycle changing the handedness of the product formed (up to 60 % Δee).

Whether or not an object has a superimposable mirror image is formally a binary issue.[1] Often, however, it is the extent to which chirality is expressed on the space surrounding a key region of a molecular structure that is important for the effective transmission of asymmetry.[2] Fledgling artificial molecular machines have been developed[3] that can transfer sequence[4] and polydispersity[5] information through to products, and that can be programmed to stereoselectively deliver different outcomes[6] when promoting successive chemical reactions. Enantiodivergent asymmetric catalysis has been demonstrated with solvent-responsive helical polymers,[7] redox-sensitive metal complexes[8] and overcrowded alkene rotary motors[9].[10-12] The trapping of a macrocycle to one side of a prochiral center with a steric barrier (a form of atropisomerism[13]) has previously been used[14] to break symmetry[15] and induce mechanical point-chirality[16] in rotaxanes. We reasoned that combining an extension of the latter principle with the controllable change of macrocycle position possible in stimuli-responsive molecular shuttles[17] could provide a strategy for achieving dynamic control over the effective "handedness" of the chiral space around a catalytic site on a rotaxane axle.[18,19] This could, in principle, be used to switch the enantioselectivity of the product formed from asymmetric catalysis with a rotaxane-based molecular machine.

Rotaxane **1** and free thread **2** are shown in Figure 1. The central region of the axle contains a 2,5-disubstituted pyrrolidine unit (red) with a pyridyl-acyl hydrazone[20] (*E*- and *Z*- colored purple and orange, respectively) to one side and a glycine amide (green) to the other.[21] The pyridyl-acyl hydrazone and glycyl amide groups are binding sites for the benzylic amide macrocycle in rotaxane *E*/*Z*-**1**, with the pyridyl-acyl hydrazone the preferred binding site in *E*-**1** and the glycyl amide group the preferred binding site in *Z*-**1**.[22]

Compounds *E*- and *Z*-**2** can be considered pseudo-*meso*[23] structures due to the symmetrical local environment of the central region of the axle (Figure 1a). In contrast, in rotaxanes *E*-**1** and *Z*-**1** the macrocycle breaks the local symmetry of the pyrrolidine unit in opposite senses according to its thermodynamically preferred position on the axle (Figure 1b). Binding to the *E*-acyl hydrazone locates the macrocycle close to the (*R*)-chiral center of the pyrrolidine ring (Figure 1b); we term this form "enhanced-(*R*)" as the macrocycle projects additional steric bulk and the potential for other types of non-covalent interactions into the space around the pyrrolidine nitrogen atom from the direction of the (*R*)-center. Binding of the macrocycle to the glycyl amide (the preferred co-conformer[24] in *Z*-**1**) changes the stereoelectronic environment in a similar way but from the perspective of the opposite (*S*)-chiral center (Figure 1b). As the binding co-conformations of benzylic amide macrocycles with pyridyl-*E*-acyl hydrazones[22] and glycyl amides[21b-d] are structurally quite similar, the enhanced-(*R*) and enhanced-(*S*) co-conformers should provide environments around the pyrrolidine nitrogen atom of fairly similar shape but of opposite handedness. To break local symmetry in this way it is unnecessary to restrict the macrocycle to different regions of the thread with a kinetic barrier,[14] and the advantage in not doing so is that it should be possible to dynamically switch between the pseudo-enantiomeric enhanced-(*R*) and enhanced-(*S*) forms of the rotaxane organocatalyst.

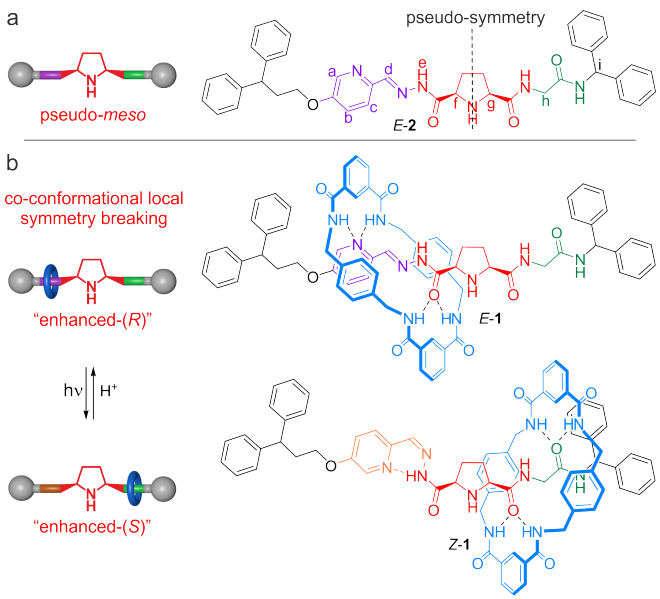

Figure 1. Structures of (a) thread **2** and (b) rotaxane **1**. The 2,5-substituted pyrrolidine unit (red) of **2** is locally symmetric, with the symmetry only broken four bond lengths in either direction from the pyrrolidine nitrogen atom, a potential active site for organocatalysis. In rotaxane **1** the space around the pyrrolidine nitrogen changes effective handedness according to the position of

[*] Dr. M. Dommaschk, J. Echavarren, Prof. D. A. Leigh, Dr. V. Marcos, Dr. T. A. Singleton
School of Chemistry, University of Manchester
Oxford Road, Manchester M13 9PL (UK)
E-mail: david.leigh@manchester.ac.uk
Homepage: http://www.catenane.net

Supporting information for this article is given via a link at the end of the document.

10.1002/anie.201908330

WILEY-VCH

COMMUNICATION

the macrocycle: in *E*-**1** the major co-conformer has the macrocycle encapsulating the *E*-acyl hydrazone (purple) adjacent to the (*R*)-stereocenter ("enhanced-(*R*)" pseudo-enantiomer); in *Z*-**1** the major co-conformer has the macrocycle encapsulating the glycine amide group (green) adjacent to the (*S*)-stereocenter ("enhanced-(*S*)" pseudo-enantiomer). Conditions: *E*-**1** to *Z*-**1**: 300 nm, 5 mW/cm^2, CH_2Cl_2, 60 min, 95 %. *Z*-**1** to *E*-**1**: 0.1 vol% CF_3CO_2H, CH_2Cl_2, 30 min, then Et_3N (0.2 vol%), quantitative.

Thread *E*-**2** and rotaxane *E*-**1** were obtained in 8 and 9 steps, respectively (see Supporting Information, Scheme S3). The key rotaxane-forming reaction to form *E*-**1**, a five-component 'clipping' macrocyclization of isophthaloyl dichloride and *p*-xylylenediamine around the pyridyl-acyl *E*-hydrazone template, proceeded in 57 % yield.[22] The *Z*-acyl hydrazone isomers, *Z*-**1** and *Z*-**2**, were each formed in 95% yield by irradiation of the corresponding *E*-rotaxane or thread with 300 nm UV-light (see Supporting Information). The downfield shift of the hydrazone NH proton (H_e; $\Delta\delta$ ~2.0 ppm, Figure 2) caused by intramolecular hydrogen bonding is characteristic of the *Z*-acyl hydrazone stereochemistry.[22] The reverse *Z*-to-*E* isomerization proceeded quantitatively with a thermal half-life of ~4 min for both **1** and **2** when triggered with 0.1% v/v trifluoroacetic acid followed by neutralization with Et_3N (Scheme 1, Figure S7).

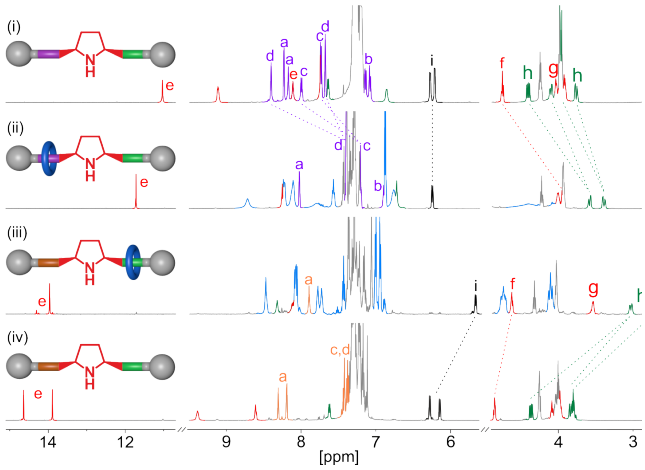

Figure 2. Partial ^{1}H NMR spectra (600 MHz, $CDCl_3$, 298 K) of (i) thread *E*-**2**; (ii) rotaxane *E*-**1**; (iii) rotaxane *Z*-**1** obtained by irradiation of *E*-**1** (300 nm, 5 mW/cm^2, CH_2Cl_2, 60 min); (iv) thread *Z*-**2** obtained by irradiation of *E*-**2** (300 nm, 5 mW/cm^2, CH_2Cl_2, 60 min). The lettering and color assignments correspond to those shown in Figure 1.

The position of the macrocycle on the axle of the rotaxanes was determined by ^{1}H NMR spectroscopy. Both hydrazone stereoisomers of the free thread, *E*-**2** and *Z*-**2**, are ~1:1 mixtures of rotamers due to slow rotation of the acyl hydrazone OC–NH bond (Figure 2 i and iv and Scheme S1). However, rotaxane *E*-**1** exists predominantly as a single rotamer (Figure 2 ii) as only one hydrazone configuration maximizes the number of strong intercomponent hydrogen bonds. The upfield shift of the pyridine and CH hydrazone protons (H_a-H_d, $\Delta\delta$ = -0.2 to -1.0 ppm) together with pyrrolidine proton H_f ($\Delta\delta$ = -0.8 ppm) confirm the encapsulation of the pyridyl *E*-acyl hydrazone by the macrocycle. Modest upfield shifts in the H_h protons result from their proximity in space to an aromatic ring of the macrocycle (Figure S9). The lack of a chemical shift change in H_i confirms the macrocycle does not circumscribe the glycyl unit.

In contrast, the significant upfield shifts of the H_i and H_h protons in *Z*-**1** with respect to *Z*-**2** ($\Delta\delta H_i$ = -0.5 and -0.9 ppm; $\Delta\delta H_h$ = -0.75 and -1.31 ppm) indicate that the macrocycle is positioned over the glycine amide unit in *Z*-**1**,[22] with small shifts in some of the pyridyl acyl hydrazone protons again a result of close proximity to the macrocycle. The chemical shifts changes are very similar to those of a previous pyridyl-acyl hydrazone shuttle showing excellent positional integrity in each rotaxane state.[22]

Having established that the macrocycle can be selectively switched between the different sides of the pyrrolidine unit in rotaxane **1**, we investigated the effectiveness of the local symmetry breaking in influencing the enantioselectivity of a catalyzed reaction, namely the enamine-mediated conjugate addition of aldehydes **3a**-**3c** to a vinyl bis-sulfone **4** (Scheme 1).[25]

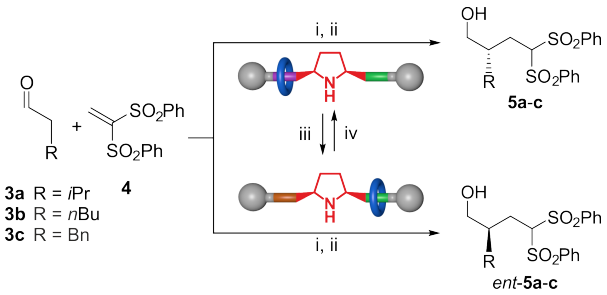

Scheme 1. Asymmetric catalysis of the enamine-mediated conjugate addition of aldehydes **3a-c** to vinyl sulfone **4**. Reagents and conditions: (i) **3a-3c** (0.1 M), **4** (0.05 M), *E*/*Z*-**1** or *E*/*Z*-**2** (5 mM), $CDCl_3$ (0.4 mL), r.t., 1-8 h; (ii) EtOH (1 mL), $NaBH_4$ (excess), 0 °C, 30 min; (iii) UV light, 300 nm, 5 mW/cm^2, 60 min; (iv) Trifluoroacetic acid (0.1 vol%), then Et_3N (0.2 vol%).

A loading of 10 mol% of rotaxane **1** or thread **2** proved sufficient to achieve high conversions (94-97%) in 1-8 hours at room temperature in chloroform (Supporting Information, Section S4). The progress of the reactions was monitored by ^{1}H NMR spectroscopy (Figure S2). The resulting aldehydes were reduced with $NaBH_4$ to the corresponding alcohols (**5a-c**) *in situ* to avoid racemization during work up, and separated by chiral HPLC.[25] The results are shown in Table 1 (see Supporting information, Figures S3-S5 and Tables S1-S3).

As anticipated, both the *E*- and *Z*-stereoisomers of the pseudo-*meso* thread **2** gave poor enantioselectivities in the catalyzed reactions. Enantiomeric excesses (ee's) of 2-6% were generated using *E*-**2** (Table 1, entries 3, 7 and 11) and 6-14% with *Z*-**2** (Table 1, entries 4, 8 and 12). In each case the small ee's produced by *E*-**2** and *Z*-**2** were in favor of the same product enantiomer.

The corresponding rotaxanes show significant improvement in their performance as asymmetric catalysts.[18g] The presence of the macrocycle on the axle increases the ee from 2-6% using pseudo-*meso* *E*-**2** to 24-40% using enhanced-(*R*) rotaxane catalyst *E*-**1** (Table 1, entries 1, 5 and 9). The position of the macrocycle breaks the pseudo-symmetry of the pyrrolidine unit, effectively projecting out from the (*R*)-stereocenter into the space around the pyrrolidine nitrogen atom. Rotaxane *Z*-**1** shows more modest increases in ee's: from 6-14% with *Z*-**2** to 16-20% using *Z*-**1** (Table 1, entries 2, 6 and 10). Significantly, however, in every

10.1002/anie.201908330

WILEY-VCH

COMMUNICATION

case the *Z*-form of the rotaxane favors the formation of the opposite enantiomer to that favored by the *E*- rotaxane: switching the position of the macrocycle from one side of the pyrrolidine unit to the other reverses the enantioselectivity of the catalyst. The greatest difference in enantioselectivities occurs with hexanal (**3b**) as the substrate, with switching the rotaxane catalyst from the enhanced-(*R*) to the enhanced-(*S*) form (i.e. *E*-**1** to *Z*-**1**) resulting in Δee of 60% for the product alcohol **5b** (Table 1, entries 5 and 6). The lower ee's generated by the *Z*-rotaxane are likely a reflection of the pseudo-*meso* threads *E*- and *Z*-**2** both favoring the formation of the same product enantiomers as *E*-**1**. Similar but less pronounced switching of ee is observed by iminium activation (Section S4.2).

Table 1. Enamine-mediated conjugate addition of aldehydes **3a-c** to vinyl sulfone **4** using catalysts **1** and **2**.

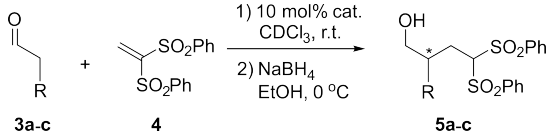

Entry[a]	Aldehyde	Catalyst		ee of 5[b]
1		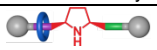	*E*-**1**	(*R*) 38
2		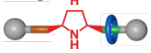	*Z*-**1**	(*S*) 18
3	**3a**	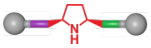	*E*-**2**	(*R*) 2
4		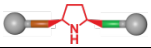	*Z*-**2**	(*R*) 6
5		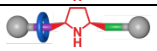	*E*-**1**	**(*S*) 40**
6		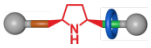	*Z*-**1**	**(*R*) 20**
7	**3b**	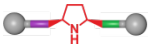	*E*-**2**	(*S*) 6
8		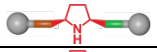	*Z*-**2**	(*S*) 14
9		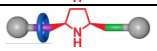	*E*-**1**	(*S*) 24
10	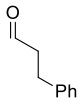		*Z*-**1**	(*R*) 16
11	**3c**	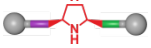	*E*-**2**	(*S*) 4
12		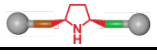	*Z*-**2**	(*S*) 14

[a] Reaction conditions as shown in Scheme 1. [b] ee's were determined by chiral HPLC and the absolute configuration assigned based on literature precedent.[25b]

In conclusion, a new principle of using the position of a macrocycle to break local pseudo-symmetry in a rotaxane axle has been demonstrated. Controlled dynamic switching allows the enantioselectivity of a rotaxane-catalyzed reaction to be reversed, enabling enantiodivergent catalysis to be achieved with a single switchable rotaxane catalyst. The ee's are relatively modest in this first example based on linear displacement symmetry-breaking (20-40 % ee for each handedness of product **5b**; cf. 50-54 % ee with the first overcrowded-alkene rotary catalysts[9a]). Nevertheless, the strategy was shown to (i) enhance the effective asymmetry,[18g] and (ii) switch the apparent handedness, of the environment around a catalytic site in a rotaxane-based molecular shuttle. A particular advantage of the concept is that it should be broadly applicable to other rotaxane systems, including designs featuring more than one ring and catalytic center or axles with a *pseudo*-prochiral center rather than *pseudo*-meso stereochemistry. Strategies that combine chemical, geometrical and dynamic design elements are likely to become increasingly important in the spatio-temporal control of chemical transformations with compound molecular machines.[26]

Acknowledgements

We thank the Engineering and Physical Sciences Research Council (EPSRC; EP/P027067/1) and the EU (European Research Council (ERC) Advanced Grant no. 786630; H2020 project Euro-Sequences, H2020-MSCA-ITN-2014, Grant no. 642083) for funding and the University of Manchester Mass Spectrometry Service Centre for high-resolution mass spectrometry. D.A.L. is a Royal Society Research Professor.

Keywords: molecular machines • rotaxanes • switchable catalysts • chirality • asymmetric catalysis

[1] M. Francl, *Nat. Chem.* **2019**, *11*, 597–598.
[2] A. F. Zahrt, S. E. Denmark, *Tetrahedron* **2019**, *75*, 1841–1851.
[3] a) E. R. Kay, D. A. Leigh *Angew. Chem. Int. Ed.* **2015**, *54*, 10080–10088; *Angew. Chem.* **2015**, *127*, 10218–10226; b) B. L. Feringa, *Angew. Chem. Int. Ed.* **2017**, *56*, 11060–11078; *Angew. Chem.* **2017**, *129*, 11206–11226; c) J.-P. Sauvage, *Angew. Chem. Int. Ed.* **2017**, *56*, 11080–11093; *Angew. Chem.* **2017**, *129*, 11228–11242; d) J. F. Stoddart, *Angew. Chem. Int. Ed.* **2017**, *56*, 11094–11125; *Angew. Chem.* **2017**, *129*, 11244–11277; e) D. A. Leigh, *Angew. Chem. Int. Ed.* **2016**, *55*, 14506–14508; *Angew. Chem.* **2016**, *128*, 14722–14724.
[4] a) B. Lewandowski, G. De Bo, J. W. Ward, M. Papmeyer, S. Kuschel, M. J. Aldegunde, P. M. E. Gramlich, D. Heckmann, S. M. Goldup, D. M. D'Souza, A. E. Fernandes, D. A. Leigh, *Science* **2013**, *339*, 189–193; b) G. De Bo, S. Kuschel, D. A. Leigh, B. Lewandowski, M. Papmeyer, J. W. Ward, *J. Am. Chem. Soc.* **2014**, *136*, 5811−5814; c) G. De Bo, M. A. Y. Gall, M. O. Kitching, S. Kuschel, D. A. Leigh, D. J. Tetlow, J. W. Ward, *J. Am. Chem. Soc.* **2017**, *139*, 10875−10879.
[5] G. De Bo, M. A. Y. Gall, S. Kuschel, J. De Winter, P. Gerbaux, D. A. Leigh, *Nat. Nanotechnol.* **2018**, *13*, 381–385.
[6] a) T. R. Kelly, M. L. Snapper, *Nature* **2017**, *549*, 336–337; b) S. Kassem, A. T. L. Lee, D. A. Leigh, V. Marcos, L. I. Palmer, S. Pisano, *Nature* **2017**, *549*, 374–378.
[7] T. Yamamoto, T. Yamada, Y. Nagata, M. Suginome, *J. Am. Chem. Soc.* **2010**, *132*, 7899–7901.
[8] S. Mortezaei, N. R. Catarineu, J. W. Canary, *J. Am. Chem. Soc.* **2012**, *134*, 8054–8057.
[9] a) J. Wang, B. L. Feringa, *Science* **2011**, *331*, 1429–1432; b) M. Vlatković, L. Bernardi, E. Otten, B. L. Feringa, *Chem. Commun.* **2014**, *50*, 7773–7775; c) D. Zhao, T. M. Neubauer, B. L. Feringa, *Nat. Commun.* **2015**, *6*, 6652.
[10] a) V. Blanco, D. A. Leigh, V. Marcos, *Chem. Soc. Rev.* **2015**, *44*, 5341–5370; b) M. Vlatković, B. S. L. Collins, B. L. Feringa, *Chem.—Eur. J.* **2016**, *22*, 17080–17111; c) N. Pairault, J. Niemeyer, *Synlett* **2018**, *29*, 689–698; d) L. van

Dijk, M. J. Tilby, R. Szpera, O. A. Smith, H. A. P. Bunce, S. P. Fletcher, *Nat. Rev. Chem*. **2018**, *2*, 0117.

[11] A change in macrocycle position has been used to block or expose catalytic sites on rotaxane axles: a) V. Blanco, A. Carlone, K. D. Hänni, D. A. Leigh, B. Lewandowski, *Angew. Chem. Int. Ed.* **2012**, *51*, 5166–5169; *Angew. Chem.* **2012**, *124*, 5256–5259; b) V. Blanco, D. A. Leigh, U. Lewandowska, B. Lewandowski, V. Marcos, *J. Am. Chem. Soc.* **2014**, *136*, 15775–15780; c) J. Beswick, V. Blanco, G. De Bo, D. A. Leigh, U. Lewandowska, B. Lewandowski, K. Mishiro, *Chem. Sci.* **2015**, *6*, 140–143; d) C.-S. Kwan, A. S. C. Chan, K. C.-F. Leung, *Org. Lett*. **2016**, *18*, 976–979; e) K. Eichstaedt, J. Jaramillo-Garcia, D. A. Leigh, V. Marcos, S. Pisano, T. A. Singleton, *J. Am. Chem. Soc.* **2017**, *139*, 9376–9381; f) J. Y. C. Lim, N. Yuntawattana, P. D. Beer, C. K. Williams, *Angew. Chem. Int. Ed.* **2019**, *58*, 6007–6011; *Angew. Chem.* **2019**, *131*, 6068–6072; g) C. Biagini, S. D. P. Fielden, D. A. Leigh, F. Schaufelberger, S. Di Stefano, D. Thomas, *Angew. Chem. Int. Ed.* **2019**, *58*, 9876–9880; *Angew. Chem.* **2019**, *131*, 9876–9880.

[12] For other examples of molecular machine designs for switchable catalysis, see: a) B. A. F. Le Bailly, L. Byrne, J. Clayden, *Angew. Chem. Int. Ed.* **2016**, *55*, 2132–2136; *Angew. Chem.* **2016**, *128*, 2172–2176; b) N. Mittal, S. Pramanik, I. Paul, S. De, M. Schmittel, *J. Am. Chem. Soc.* **2017**, *139*, 4270–4273; c) G. De Bo, D. A. Leigh, C. T. McTernan, S. Wang, *Chem. Sci.* **2017**, *8*, 7077–7081.

[13] E. L. Eliel, S. H. Wilen, *Stereochemistry of Organic Compounds*, Wiley, New York, **1994**.

[14] a) M. Alvarez-Pérez, S. M. Goldup, D. A. Leigh, A. M. Z. Slawin, *J. Am. Chem. Soc*. **2008**, *130*, 1836–1838; b) A. Carlone, S. M. Goldup, N. Lebrasseur, D. A. Leigh, A. Wilson, *J. Am. Chem. Soc*. **2012**, *134*, 8321–8323; c) Y. Cakmak, S. Erbas-Cakmak, D. A. Leigh, *J. Am. Chem. Soc*. **2016**, *138*, 1749–1751.

[15] a) N. H. Evans, *Chem.—Eur. J.* **2018**, *24*, 3101–3112; b) E. M. G. Jamieson, F. Modicom, S. M. Goldup, *Chem. Soc. Rev*. **2018**, *47*, 5266–5311.

[16] Classified as 'co-conformationally covalent point/centrally chiral' in ref [15b].

[17] a) R. A. Bissell, E. Córdova, A. E. Kaifer, J. F. Stoddart, *Nature,* **1994**, *369*, 133–136; b) A. S. Lane, D. A. Leigh, A. Murphy, *J. Am. Chem. Soc.* **1997**, *119*, 11092–11093; c) H. Tian, Q.-C. Wang, *Chem. Soc. Rev*. **2006**, *35*, 361–374; d) S. Erbas-Cakmak, D. A. Leigh, C. T. McTernan, A. L. Nussbaumer, *Chem. Rev*. **2015**, *115*, 10081–10206.

[18] For examples of enantioselective catalysis by chiral interlocked molecules, see: a) Y. Tachibana, N. Kihara, T. Takata, *J. Am. Chem. Soc.* **2004**, *126*, 3438–3439; b) Y. Tachibana, N. Kihara, K. Nakazono, T. Takata, *Phosphorus, Sulfur Silicon Relat. Elem.* **2010**, *185*, 1182–1205; c) V. Blanco, D. A. Leigh, V. Marcos, J. A. Morales-Serna, A. L. Nussbaumer, *J. Am. Chem. Soc.* **2014**, *136*, 4905–4908; d) S. Hoekman, M. O. Kitching, D. A. Leigh, M. Papmeyer, D. Roke, *J. Am. Chem. Soc.* **2015**, *137*, 7656–7659; e) Y. Cakmak, S. Erbas-Cakmak, D. A. Leigh, *J. Am. Chem. Soc.* **2016**, *138*, 1749–1751; f) F. Ishiwari, K. Nakazono, Y. Koyama, T. Takata, *Angew. Chem. Int. Ed.* **2017**, *56*, 14858–14862; *Angew. Chem.* **2017**, *129*, 15054–15058; g) A. Martinez-Cuezva, M. Marin-Luna, D. A. Alonso, D. Ros-Ñiguez, M. Alajarin, J. Berná, *Org. Lett.* **2019**, *21*, 5192–5196. For the use of a chiral [2]catenane in enantioselective catalysis, see: h) R. Mitra, H. Zhu, S. Grimme, J. Niemeyer, *Angew. Chem. Int. Ed.* **2017**, *56*, 11456–11459; *Angew. Chem.* **2017**, *129*, 11614–11617. For the use of a topologically chiral trefoil knot in enantioselective catalysis, see: i) G. Gil-Ramírez, S. Hoekman, M. O. Kitching, D. A. Leigh, I. J. Vitorica-Yrezabal, G. Zhang, *J. Am. Chem. Soc.* **2016**, *138*, 13159–13162.

[19] For examples of diastereoselective catalysis by chiral rotaxanes, see: a) M. Galli, J. E. M. Lewis, S. M. Goldup, *Angew. Chem. Int. Ed.* **2015**, *54,* 13545–13549; *Angew. Chem.* **2015**, *127*, 13749–13753; b) A. Martinez-Cuezva, C. Lopez-Leonardo, D. Bautista, M. Alajarin, J. Berná, *J. Am. Chem. Soc.* **2016**, *138*, 8726–8729; c) A. Martinez-Cuezva, A. Saura-Sanmartin, T. Nicolas-Garcia, C. Navarro, R.-A. Orenes, M. Alajarin, J. Berná, *Chem. Sci.* **2017**, *8*, 3775–3780; d) A. Martinez-Cuezva, D. Bautista, M. Alajarin, J. Berná, *Angew. Chem. Int. Ed.* **2018**, *57*, 6563–6567; *Angew. Chem.* **2018**, *130*, 6673–6677.

[20] a) M. N. Chaur, D. Collado, J.-M. Lehn, *Chem.—Eur. J.* **2011**, *17*, 248–258; b) G. Vantomme, N. Hafezi, J.-M. Lehn, *Chem. Sci.* **2014**, *5*, 1475–1483; c) D. J. van Dijken, P. Kovaříček, S. P. Ihrig, S. Hecht, *J. Am. Chem. Soc.* **2015**, *137*, 14982–14991. For selected examples of the use of hydrazones in molecular machines, see: d) X. Su, I. Aprahamian, *Org. Lett.* **2011**, *13*, 30–33; e) X. Su, T. F. Robbins, I. Aprahamian, *Angew. Chem. Int. Ed.* **2011**, *50*, 1841–1844; *Angew. Chem.* **2011**, *123*, 1881–1884; f) D. Ray, J. T. Foy, R. P. Hughes, I. Aprahamian, *Nat. Chem.* **2012**, *4*, 757–762; g) S. Kassem, A. T. L. Lee, D. A. Leigh, A. Markevicius, J. Solà, *Nat. Chem.* **2016**, *8*, 138–143; h) Q. Li, H. Qian, B. Shao, R. P. Hughes, I. Aprahamian, *J. Am. Chem. Soc*. **2018**, *140*, 11829–11835; i) A. Blanco-Gómez, A. Fernández-Blanco, V. Blanco, J. Rodríguez, C. Peinador, M. D. García, *J. Am. Chem. Soc.* **2019**, *141*, 3959–3964; j) B. Shao, H. Qian, Q. Li, I. Aprahamian, *J. Am. Chem. Soc*. **2019**, *141*, 8364–8371; k) Y.-X. Yuan, Y.-S. Zheng, *ACS Appl. Mater. Interfaces* **2019,** *11*, 7303–7310.

[21] For a recent review on amide catenanes and rotaxanes, see: a) N. H. Evans, *Eur. J. Org. Chem*. **2019**, 3320–3343.

[22] D. A. Leigh, V. Marcos, T. Nalbantoglu, I. J. Vitorica-Yrezabal, F. T. Yasar, X. Zhu, *J. Am. Chem. Soc.* **2017**, *139*, 7104–7109.

[23] a) B. M. Trost, *Acc. Chem. Res*. **1996**, *29*, 355–364; b) R. Stranne, J.-L. Vasse, C. Moberg, *Org. Lett.* **2001**, *3*, 2525–2528.

[24] 'Co-conformation' refers to the relative positions of noncovalently linked components with respect to each other, see: M. C. T. Fyfe, P. T. Glink, S. Menzer, J. F. Stoddart, A. J. P. White, D. J. Williams, *Angew. Chem. Int. Ed. Engl.* **1997**, *36*, 2068–2070; *Angew. Chem.* **1997**, *109*, 2158–2160.

[25] a) S. Mossé, A. Alexakis, *Org. Lett*. **2005**, *7*, 4361–4364; b) A. Landa, M. Maestro, C. Masdeu, Á. Puente, S. Vera, M. Oiarbide, C. Palomo, *Chem.—Eur. J.* **2009**, *15*, 1562–1565.

[26] L. Zhang, V. Marcos, D. A. Leigh, *Proc. Natl. Acad. Sci. USA* **2018**, *115*, 9397–9404.

10.1002/anie.201908330

WILEY-VCH

COMMUNICATION

Entry for the Table of Contents

COMMUNICATION

Changing hands. Leigh et al use the stimuli-induced change of macrocycle position in a rotaxane to switch the effective handedness of a catalytic center on the axle. The dynamic switching is used to reverse the enantioselectivity of an enamine-mediated conjugate addition.

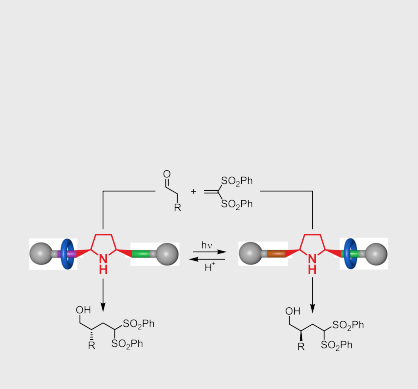

M. Dommaschk, J. Echavarren, D. A. Leigh, V. Marcos, T. A. Singleton*

Page No. – Page No.

Dynamic Control of Chiral Space Through Local Symmetry Breaking in a Rotaxane Organocatalyst